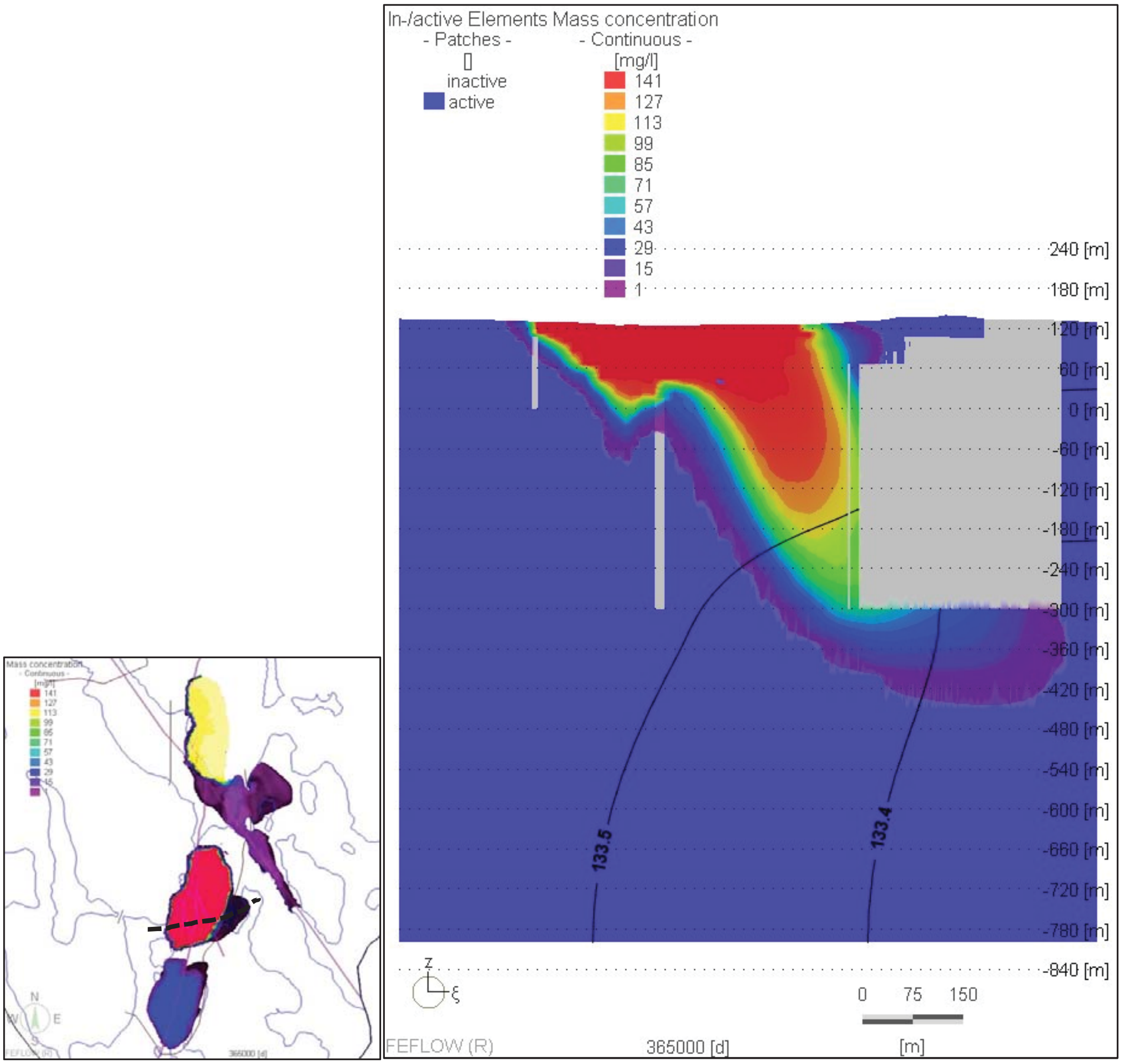

Figure 30 : Vertical section of predicted chloride concentrations from Pit E, 1000 years after in-pit deposition

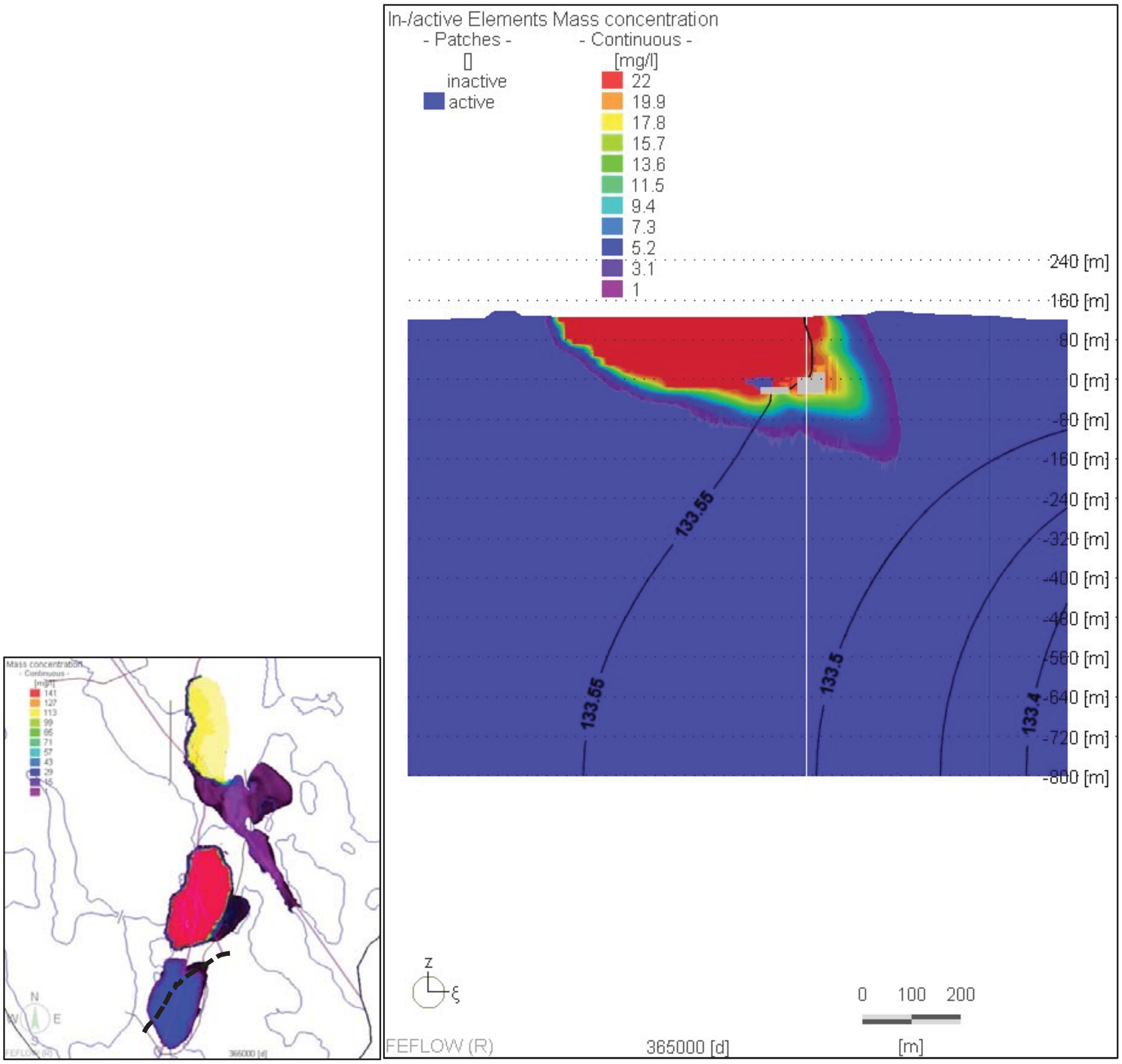

Figure 31 : Vertical section of predicted chloride concentrations from Goose Pit, 1000 years after in-pit deposition

Each chemical species will have a different behavior in the groundwater, but the chloride plume shows a relevant example of how the groundwater gradient, dispersion and porosity can affect the transport of a contaminant. Regardless of initial concentrations and CCME guideline of other chemical species, chloride represents a worst case scenario for the transport velocity since it is a non-reactive compound and acts as a tracer.

4.3.2 Arsenic

In order to appreciate the impact of adsorption on the transport of dissolved arsenic, arrival times of retarded and non-retarded arsenic were compared.

First, transport of arsenic was simulated without a retardation factor in order to establish the non-retarded velocity of the contaminant between Pit A and East Dike. Simulation results (Figure 32) show that non-retarded arsenic will exceed the CCME guideline (0.005 mg/L) at East Dike after 235 years of simulation.

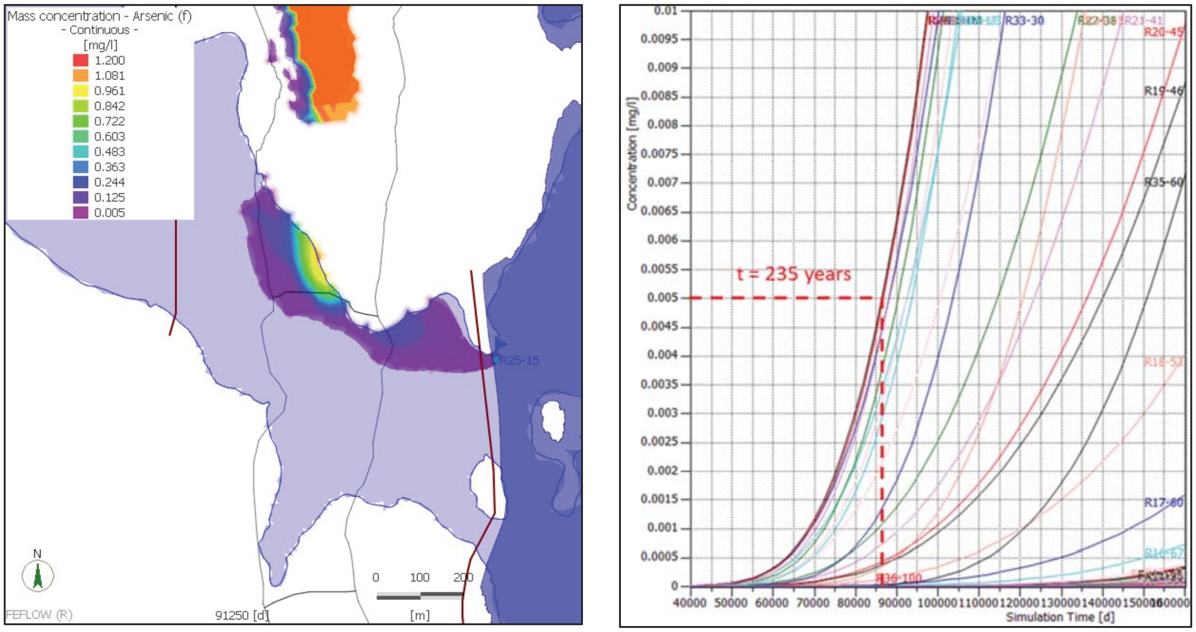

Figure 32 : Plume distribution on first breakthrough of the 0.005 mg/L isocontour of arsenic at East Dike after 235 years

Then, based on the following equation, the calculated retardation factor for arsenic is R = 391 501.

$$R = 1 + \frac{\rho_b}{\theta} * K_d, \quad \text{with, } \rho_b = 2.7\ \text{g/cm}^3,\ K_d = 29\ \text{L/kg and } \theta_{eff} = 0.0002.$$

With this method, the value of the retardation factor R suggests that arsenic would travel 391 501 times slower than groundwater, which means that the first time arrival, presented in Table 10, is almost equal to 100 million years. Practically, this would means that arsenic will be stationary. Indeed, since the water velocity in the model is already very low ($8.7\text{x}10^{-8}$ m/s), the velocity of arsenic is, in consequence, much lower ($2.2\text{x}10^{-13}$ m/s).

Table 10 : First arrival times of arsenic at East Dike considering a retardation factor

Parameter	Unit	CCME guideline	*Pit A initial concentration	K_d values (L/kg)	Retardation factor (-)	Velocity (m/s)	t (y)
Non-retarded arsenic	mg/L	0.005	0.9	0	1	8.7x10^{-8}	235
Retarded arsenic	mg/L	0.005	0.9	29	391 501	2.2x10^{-13}	Stationary state (estimated to 100 M yrs)

*Initial water quality concentrations are as predicted by the in-pit water quality assessment at closure report (SNCL, 2018a) and untreated.

4.4 Sensitivity analysis

A sensitivity analysis was completed on chloride transport because it is a non-reactive chemical compound. The following transport parameters were tested in order to appreciate the impact of the first arrival time at a chloride concentration of 1 mg/L at the location of East Dike:

> **Effective porosity**: contaminant advective migration velocity is inversely proportional to effective porosity. As shown previously, chloride from Pit A migrates faster through the bedrock under Central Dump (θ_{eff} = 0.0002) than through the Dump itself (θ_{eff} = 0.3), although the Dump is adjacent to the pit. In a conservative perspective, this parameter was thus decreased.

> **Dispersivity**: the simulation results for chloride showed how the dispersivity would lead to spreading of the plume and decrease concentration gradients. The dispersivity was increased by a factor of 4 to give a general appreciation of its sensitivity.

> **Lake levels**: simulation results showed very long migration times (over 250 years for chloride), mainly caused by a very low hydraulic gradient (locally less than 0.00005 m/m). It is expected that a more drastic difference between upstream/downstream lake levels would lead to a general increase of the groundwater gradient. Boundary conditions of the model were thus modified by lowering Second Portage Lake by two (2) meters. According to AEM data, lake levels vary from 132.4 to 133.4 masl for Second Portage Lake and from 133.1 to 134.1 masl for Third Portage Lake.

General impacts at East Dike

Table 11 shows the first arrival times of chloride at East Dike for the chloride transport base case scenario and three (3) sensitivity analysis scenarios. All parameters have significant impacts on the breakthrough time of chloride at the lake.

Table 11 : Results of sensitivity analysis on transport simulations

Scenario	Parameter	Variation	First arrival time (yrs) of chloride at East Dike (W_{ED}) considering Conc.= 1 mg/L
Base Case	n/a	n/a	255
Case 1	Effective porosity	Divided by 2	125
Case 2	Second Portage Lake level	Minus 2 m	120
Case 3	Dispersivity	Multiplied by 4	175

As expected, variations in effective porosity and lake levels, led to increased chloride velocity and thus reduced arrival times (respectively 125 and 120 years). Increasing the dispersivity also led a shorter first arrival time (175 years) compared to the base case. Actually, the impact of dispersivity is two-fold as shown in Figure 33:

- on one hand the dispersivity shortens the first arrival time because the contaminant is rapidly dispersed, so it reaches the lake faster, but
- on the other hand, since the contaminant is rapidly spread out, long-term concentrations will be almost 10 mg/L lower than the base case (71 mg/L versus 79 mg/L, for Case 3 and the Base Case respectively).

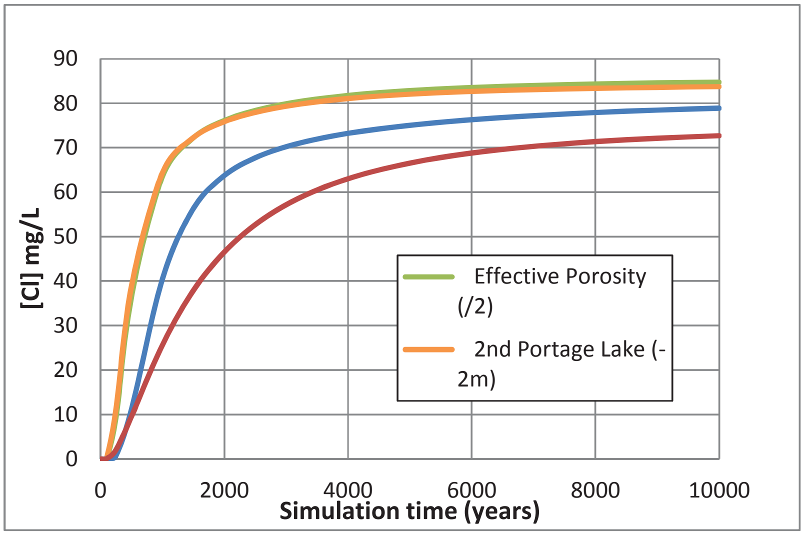

Figure 33 : Evolution of simulated concentrations with time at W_{ED} (z = 15 masl) for the sensitivity analysis scenarios

Specific impacts from reducing Second Portage Lake level

Porosity and dispersivity affects the concentration gradient of the chloride plume, but the general shape remains similar to the base case. On the contrary, since it modifies the groundwater flow pattern, the variation of lake levels significantly changed the shape of the plume. Based on Figure 34b, which presents long term concentrations considering the variation in lake level, the following observations are made:

> Chloride from Portage Pit E migrates northwards through the thawed permafrost zone located on the upper border of Pit E;

> Portage Pit E and Goose Pit plumes reach the outflow border of the model, after resurfacing from beneath the permafrost;

> Pit A plume shape remains similar to the base case but migration velocity is higher.

Case 2 is considered a worst case scenario since it would be almost impossible for Second Portage Lake and Third Portage Lake to have such difference in hydraulic heads.

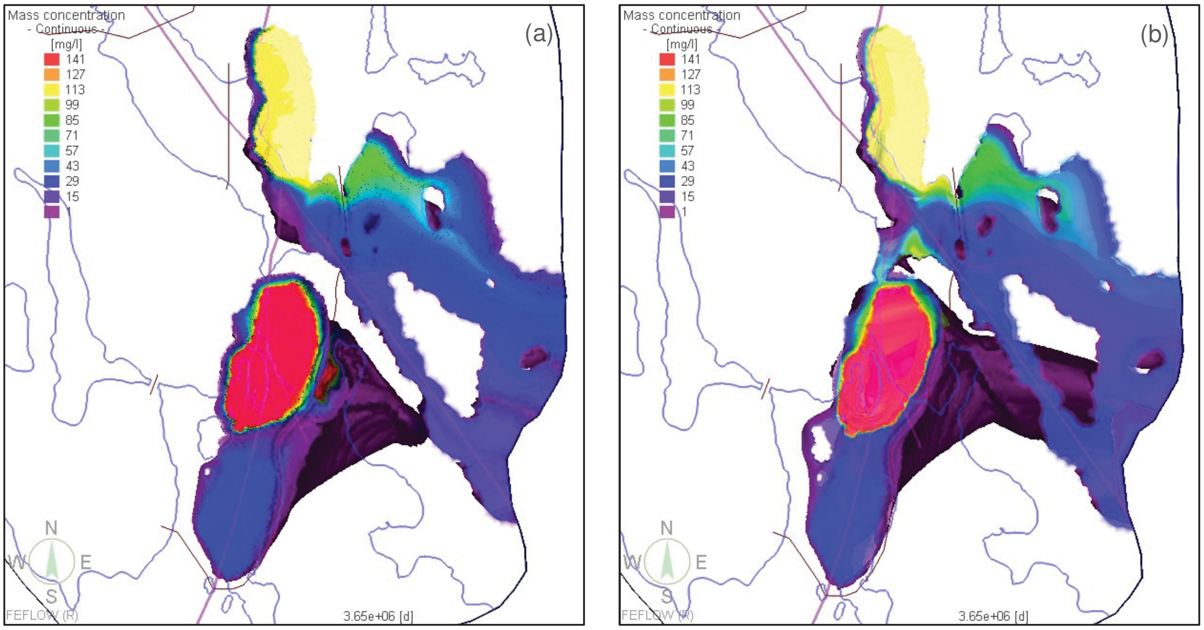

Figure 34 : Long-term pattern of chloride plumes after 10,000 years for (a) the base case and (b) considering a reduction of Second Portage Lake level by 2 m

5.0 LIMITATIONS

The following limitations are acknowledged in the numerical hydrogeological modelling:

- Many aspects of the conceptual model are not possible to represent in the numerical model, because the hydrogeological systems are very complex. A conceptual model gives the basic idea or constructed understanding of how systems and processes operate (Bredehoeft, 2005).
- The model is a simplification of the significant variability of the hydraulic conductivities and hydrostratigraphic units and does not include preferential flow that would occur in the discrete bedrock fractures and till deposit. Hydraulic conductivity has been represented by horizontal layers;
- Fracture connectivity and distribution remain unknown over the model extent, including near the pits. This is one reason why an equivalent porosity model, instead of a complex discrete fracture model, has been used for this study;
- Due to seasonal variations in the groundwater regime, there is a large variability in pit pumping rates. Thus, the model was calibrated using annual measured pumping rates from 2016 to reduce seasonal effects and inter-season water storage in snow or ice walls within the pits.
- The thermally active (thawed) zone and associated runoff were not represented in the model;
- Permafrost degradation was simulated over 100 years after in-pit tailings deposition. Predictions over this timeframe will not make sense based on uncertainties and constant revision of global warming scenarios.
- There is no hydrogeological information available below 200 m depth (hydraulic conductivity, ground temperature data, piezometric data). Therefore, the vertical extent of hydraulic conductivities, faults and permafrost has been extrapolated based on data and comprehension of the system. However, it was possible to represent the deep groundwater flow regime;
- The deep groundwater flow gradient is based on surrounding arithmetic mean lake elevations instead of on deep groundwater piezometric information. During dewatering and calibration process, the south end of Central Dump was considered in the permafrost zone without a hydraulic connection between Second Portage Lake arm and Portage Pit E. A limited dewatering rate at Portage Pit E suggests that this assumption is reliable.
- To validate the model, the results from the simulation need to be compared with observations from field, but the calibration for mass transport was not possible with available data.
- Although K_d model is an integral part of current methodologies for modelling contaminant and risk analysis, in this context, this method shows how it could lead to an important retardation factor. Hence, for most situations that is sensitive to the selected K_d value, site-specific K_d values are essential for obtaining defensible risk and transport predictions (EPA, 1999).
- As mentioned by the EPA (2004), site-specific K_d values should be measured for the range of aqueous and geological conditions in the system to be modeled. However, literature-derived K_d values are commonly used for screening calculations. Suitable selection and use of literature-derived K_d values for screening calculations of contaminant transport is not a trivial matter. Among the assumptions implicit with the K_d construct is: (1) only trace amounts of contaminants exist in the aqueous and solid phases, (2) the relationship between the amount of contaminant in the solid and liquid phases is linear, (3) equilibrium conditions exist, (4) equally rapid adsorption and desorption kinetics exists, (5) it describes contaminant partitioning between one sorbate (contaminant) and one

sorbent (soil), and (6) all adsorption sites are accessible and have equal adsorption binding energies. Many of these assumptions are not met for groundwater/soil environments. Thus, literature-derived K_d values should be used with caution only to predict transport in systems similar to those used in the laboratory and field to measure the K_d. Variation in either the soil or aqueous chemistry of a system can result in extremely large differences in K_d values.

6.0 CONCLUSIONS

Agnico Eagle Mines Limited (AEM) is planning to develop the Whale Tail Pit, a satellite deposit on Amaruq property, as a continuation of mine operations and milling at the Meadowbank Mine. After a multi-account analysis, in-pit tailings deposition (IPD) was selected as the preferred option to store tailings waste produced from the Whale Tail Mine. A prefeasibility study was conducted to develop a 3D hydrogeological numerical model to assess potential contaminant transport from in-pit tailings disposed in Portage Pit A, Pit E and Goose Pit. Field work has also been carried out to refine hydrogeological context of potential seepage areas. This Detailed Engineering Study is in continuity with the last Prefeasibility Study (PFS) (SLI, 2018) and has presented the updated 3D hydrogeological model work. Main objective of the hydrogeological study was to assess the contaminant migration through groundwater and the potential impact of the in-pit tailings deposition on the surrounding lakes.

In order to achieve this objective, the latest field investigation carried out during the PFS and other relevant information have been considered to update the hydrogeological and contaminant transport conceptual models, to implement geological features (quartzite/ultramafic contact and North Channel fractured zone, for example) to the 3D FEFLOW model and to update hydraulic properties such as hydraulic conductivity and porosity. Hydrogeological conceptual models were developed for two periods, e.g. one during the 2016 pits mining & dewatering operations, which was used for model calibration, and another one during the post-closure period, which was used for contaminant transport predictions. Available data and field observation of seepage areas in pit walls help develop the conceptual model.

FEFLOW software was used to represent 3D hydrogeological conditions and to perform contaminant transport simulations. Domain boundaries were set according to lake locations and elevations, and with anticipated regional groundwater flow. Over the domain consisting of 22 km^2 coverage, 4 km wide and 1 km depth, meshing with triangular prism was created with refined elements where high hydraulic gradients were anticipated, e.g. dikes and pits. Such a deep numerical model was developed to account for groundwater regional flow below permafrost extension. At Meadowbank site and inside the model domain, regional groundwater flows, in natural conditions, will flow from the northwest boundary to the southeast boundary in Second Portage Lake direction, driven by water elevation differences of open talik lakes. The permafrost lateral extension has been delineated during the prefeasibility study (SLI, 2017) assuming that the limit corresponds to the shoreline minus a 1.5 m water depth within large lakes. This assumption matches well with available thermistor data. Existing active and inactive thermistor data were also reviewed during the PFS to estimate the maximum depth of the permafrost areas. Depending on proximity to the lakes, permafrost thickness reaches about 170 m at former Goose Pit Island (on the East wall of Goose Pit) and more than 400 m (Pit A, Pit E area).

Hydraulic conductivities for each hydrostratigraphic unit were reviewed with existing data and new packer test results from the 2017 IPD field investigation. Focus has been made on bedrock properties for each unit (upper fractured bedrock, weathered bedrock, competent bedrock) and faults (Second Portage Lake Fault, Bay Fault, Bay Fault Splay, North Channel fractured zone), in which groundwater would preferably flow from the pits to the lakes at post-closure. Bedrock hydraulic conductivities were not clearly related to their lithology description. However, bedrock hydraulic conductivity was found to generally decrease with depth (from 10^{-7} m/s between 5 to 60 mbgs and to 10^{-8} m/s between 60 to 150 mbgs). No data were available below 200 mbgs but properties were inferred from the general trend of hydraulic conductivity with depth. Fault hydraulic conductivities were extracted from datasets and were typically similar to slightly higher than competent bedrock. Tailings hydraulic conductivity was based on the laboratory permeability tests performed by Golder (2017) on Amaruq's tailings. Hydraulic conductivity from other units (till, dikes, Central Dump waste rock material) has been based either on available data or literature values. Permafrost in areas were considered in the model as inactive cells, meaning that they are not permeable and do not participate to groundwater flow.

The 3D hydrogeological model was calibrated with 2016 pumping rates at Portage Pit A&E, at Central Dike downstream pond and at the two pumping wells at East Dike. Note that Goose Dike mining has stopped before 2016 and its water level rising rate has been considered equal to what would have been measured under dewatering operations. Based on winter months, where the groundwater contribution was extracted from these total rates, the groundwater contribution was estimated to be 127 m^3/d (35% of total pumping rate) at Portage Pit A&E, 435 m^3/d (42% of total pumping rate) at Goose Pit, 12 770 m^3/d at Central Dike D/S pond and 500 m^3/d at East Dike pumping wells together. Hydraulic conductivities were adjusted within reasonable ranges to simulate the observed 2016 annual groundwater contribution to the water inflow at each pit, Central Dike D/S Pond and East Dike pumping wells. Globally, faults and fractured zones hydraulic conductivities have been slightly increased (0.5 order of magnitude) and competent bedrock between 30 and 60 mbgs. Observed hydraulic heads from vibrating wire piezometers located in different areas of the mine site have been compared to the simulated heads and the root mean square error (RMSE = 9%) is in agreement with the industry standard (RMSE < 10%) and considering that observation points are located where hydraulic heads change drastically over short distance, e.g. between lakes and pit rims or dikes. Based on the sensitivity analysis on hydraulic conductivity the till and upper fractured bedrock hydraulic conductivity have a major impact on the simulated pumping rate at Central Dike D/S pond, increasing the flow rate by 1.9 times if its hydraulic conductivity is doubled. The quartzite-ultramafic contact also leads to a 1.6 times greater inflow into Goose Pit if its hydraulic conductivity is doubled. Also, the hydraulic conductivity of the small permafrost zone at the southwestern end of Portage Pit A has a great impact on simulated groundwater inflow to the same pit. Little effect on pit inflow has been seen with increases of tailings or faults hydraulic conductivity and with lake levels variation.

Contaminant transport modelling was carried out with two selected chemical components: chloride and arsenic. Chloride was selected because it is a conservative non-reactive tracer and will follow the pathway and velocity of groundwater. Dissolved arsenic was also selected for transport simulations as it is a well-known toxic compound, it is exceeding the CCME criteria at the pit source, if untreated, and it is less retarded than other metals. These two chemical parameters are typically found in reclaim water geochemical signatures. It was assumed that initial dissolved concentration of the plume source was similar to the untreated in-pit water quality assessment at closure, produced during the Detailed Engineering. Chloride and arsenic results were compared with the CCME guideline for the Long-term Aquatic Life Protection for fresh water, 120 mg/L and 0.005 mg/L, respectively.

Considering the very low hydraulic gradient and groundwater velocities at the mine site, the source concentrations were considered constant over time because it will take more than 60 000 years to flush 3 pore volumes and to reach residual concentration of the source. Initial untreated concentration of chloride in Portage Pit A, Pit E and Goose Pit would be 115, 141 and 41 mg/L respectively, as per in-pit water quality assessment at closure. Only Pit E initial untreated concentration of the pit source would exceed CCME guideline (120 mg/L). For dissolved arsenic, initial untreated concentration at the source would be 0.9, 1.1 and 0.15 mg/L at Pit A, Pit E and Goose Pit, respectively and are consequently 180, 220 and 30 times greater than its applicable criteria (0.005 mg/L).

Before transport simulations, existing data and literature review was carried out to select proper transport parameters, such as effective porosity, dispersivity, as well as partition coefficient, molecular diffusion for both chloride and arsenic. Effective porosities for bedrock have been based on an extensive review of televiewer surveys conducted in existing and new 2017 IPD boreholes, located in potential seepage paths. Note that permafrost degradation 2D TEMP/W simulations results conducted during this Detailed Engineering Study, including global warming and tailings deposition warming effects, have been integrated to the 3D hydrogeological modelling and transport predictions during post-closure period. To do so, initial inactive cells, representing permafrost areas, have been re-activated in pit shells accordingly to predict thaws.

Transport simulation results for chloride allow concluding that:

- Chloride at East Dike will never exceed the CCME criteria of 120 mg/L, because the initial untreated concentration of the Pit A source is below criteria 115 mg/L. The maximum concentration to reach East Dike will be around 85 mg/L, due to dispersion effect that will tend to spread the plume and decrease concentrations;
- Breakthrough point of 50% of the Pit A plume chloride concentration, corresponding to 40 mg/L, will reach Second Portage Lake after 1100 years;
- First appearance of chloride from Pit A will reach Second Portage Lake after 255 years with a concentration of 1 mg/L.
- For Portage Pit E and Goose Pit, the flow paths are oriented downward and dissolved compound will prefer dipping under the permafrost to reach the lowest hydraulic head point of the modeled system, e.g. Second Portage Lake. Over the simulation period (10 000 years) chloride has not reached neither Second Portage Lake, nor Third Portage Lake and thus, is considered stationary.

Transport simulations for dissolved arsenic allow concluding that:

- A non-retarded and untreated dissolved arsenic source originating from Portage Pit A would reach Second Portage Lake at the CCME criteria (0.005 mg/L) after 235 years;
- However when the arsenic partition coefficient (K_d = 29 L/kg), and calculated retardation faction (R = 391 501) are accounted, arsenic is considered stationary;
- As noticed for chloride, dissolved arsenic plume originating from Pit E and Goose Pit would migrate downward below the permafrost island.

In order to look at the transport simulations sensitivity, selected parameters were chosen to complete this analysis. Main findings are:

- Increasing the dispersivity and the hydraulic gradient to the lake, and decreasing the effective porosity, will decrease the first arrival times of the Pit A plume at East Dike;
- Increasing the dispersivity will reduce peak concentrations;
- Decreasing the level of Second Portage Lake will increase the groundwater flow velocities and locally change migration paths from Pit E and Goose Pit, but not from Pit A;

It is important to note that this modelling work was completed in a conservative perspective since:

- Contaminant concentrations at the source (tailings pore water) are considered constant over time, since it will take almost 60 000 years to flush 3 pore volumes due to a very low hydraulic gradient;
- The extent of permafrost degradation, including that due to climate change, was considered in post-closure transport simulations;
- Contaminant transport simulations do not consider any geochemical degradation effects but only apply a retardation factor; (for example, co-precipitation of arsenic with Fe(III) can also lead to significantly reduced arsenic concentrations in groundwater, Osama 2010);

REFERENCES

The following reports were consulted for this mandate:

Adams, E.E., and L.W. Gelhar. 1992. Field study of dispersion in a heterogeneous aquifer. 2: Spatial moments analysis. Water Resources Research 28(12), 3293-3307

AEM Communication (2017) Update on Central Dike Assessment. Presentation to the Meadowbank Dike Review Board. Doc 1557 – 1667025 Rev 0. March 23, 2017.

AEM (2016b). 2015 Groundwater Monitoring Report. 15 p., March 2016.

AEM (2016a). Technical Memo Central Dike Seepage Action Plan - South Cell Tailings Facilities. Summary of results and conclusion, January 10 2016, 7 p.

AEM (2015). 2014 Groundwater Monitoring Report. 16 p., March 2015.

AEM (2014a). Annual Review of Portage, Goose, and Vault Pit Slope Performance (2014) – Meadowbank Mine, 89 p., November 19, 2014

AEM (2014b). 2014 Tailings Storage Facility Investigation Program. Report V1. July 3rd, 2014.

AEM (2014c). 2013 Groundwater Monitoring Report. 12 p. January 2014.

Appelo, C. A. J. and Postma, D. (1993). Geochemistry, groundwater and pollution: Brookfield, vt., A. A. Balkema publisher, 536 p.

API (2011). Groundwater Arsenic Manual Attenuation of Naturally-Occurring Arsenic at Petroleum Impacted Sites

Awoh, A.S., 2012. Étude expérimentale du comportement géochimique de résidus miniers hautement sulfureux sous un recouvrement en eau. Ph.D. Diss. UQAT, Rouyn-Noranda, Canada. http://depositum.uqat.ca/447/

Barone, F.S., Rowe, R.K., and Quigley, R.M. (1992). Estimate of chloride diffusion coefficient and tortuosity factor for mudstone. Journal of Geotechnical Engineering, ASCE, 118: 1031-1046.

Bethke, C. M. (1996). Geochemical Reaction Modelling: Concepts and Applications, Oxford University Press, 9 mai 1996 - 416 pages

CJ Clayton Mine Geotechnical Investigation Ltd. (2015a). Meadowbank Mine - Assessment of Pit E3 South Wall Stability. Project no. PN2015-02, Doc no. RPT-001, 81 p., December 21, 2015.

CJ Clayton Mine Geotechnical Investigation Ltd. (2015b). Annual review of pit slope performance (2015). Project: PN2015-01. Document: RPT-001. November 28, 2015.

Cumberland Resources Ltd (2005a). Meadowbank Gold Project - Baseline Physical Ecosystem Report. 93 p., October 2005.

Cumberland Resources Ltd (2005b). Meadowbank Gold Project - Mine Waste & Water Management. 126 p., October, 2005.

Cumberland Resources Ltd (2003). Meadowbank Project Nunavut – Field Geotechnical Studies, September 8, 2003, 31 p.

Davis, S. N., Thompson, G. M., Bentley, H. W., Stiles, G. (1980). Ground-Water Tracers — A Short Review

Dominico, P.A., and F.W. Schwartz, (1990). Physical and Chemical Hydrogeology, John Wiley and Sons, N.Y., 824 p.

EPA (1996). Soil Screening Guidance: Technical Background Document. Second Edition. Publication 9355.4-17A. May 1996. United States Environmental Protection Agency. Office of Solid Waste and Emergency Response Washington DC 20460

EPA (2002). Calculation and Use of First-Order Rate Constants for Monitored Natural Attenuation Studies

EPA (2004). UNDERSTANDING VARIATION IN PARTITION COEFFICIENT, Kd, VALUES Volume III: Review of Geochemistry and Available Kd Values for Americium, Arsenic, Curium, Iodine, Neptunium, Radium, and Technetium

Fetter, C.W. (1999). Contaminant hydrogeology, Prentice Hall, New Jersey

Fields K, Chen A, Wang L (2000) Arsenic removal from drinking water by iron removal plants. Batelle EPA/600/R-00/086

Franz Environmental (2009). Peer Review of Monitoring Well Design to Minimize the Effects of Permafrost Damage at Agnico Eagle's Meadowbank Mine in Nunavut. 9 p., March 23, 2009.

Freeze, R.A., and Cherry, J.A., 1979, Groundwater: Englewood Cliffs, NJ, Prentice-Hall, 604 p.

Gelhar, L.W., and C.L. Axness. 1983. Three-dimensional stochastic analysis of macrodispersion in aquifers. Water Resources Research 19(1), 161-180.

Gelhar, L.W. 1986. Stochastic subsurface hydrology from theory to applications. Water Resources Res earch 22(9), 1 35S- I 45S

Gelhar, L. W., C. Welty, and K. R. Rehfeld (1992). A critical review of data on field-scale dispersion in aquifers. Water Resources Res., v.28, no. 7, p.1955-1974.

Golder Associates Ltd. (2017). Central Dike Seepage and Performance Assessment Update. Draft Report. June 2017.

Golder Associates Ltd. (2016). Evaluation of the Geochemical Properties of Waste Rock, Ore,Tailing, Overburden and Sediment from the Whale Tail Pit and Road Aggregate Materials

Golder Associates Ltd. (2015a). Evaluation of the Geochemical Properties of Waste Rock, Ore, Tailing, Overburden and Sediment from the Whale Tail Pit and Road Aggregate Materials Agnico Eagle Mines, Meadowbank Division, Report 1520817 Doc 042, November 2015.

Golder Associates Ltd. (2015b). Hydrogeological Analysis to Support South Wall Slope Stability Assessment, Meadowbank Mine Pit E3. Presented to Agnico Eagle Mines Limited October 23, 2015.Portage Pit A – Central Dike Seepage.

Golder Associates Ltd. (2012a). Dike Setback Study and East Pit Wall Stability - Goose Pit - Meadowbank Mine. Project no. 11-1221-0083/6000, Doc no. 1378 Ver. 0, 57 p. October 31, 2012.

Golder Associates Ltd. (2012b). 2012 Groundwater Monitoring and Water Quality Results - Meadowbank Mine, Nunavut. Doc no. 1386-1212210081, Ver. 0, 6 p., October 19, 2002.

Golder Associates Ltd. (2011). 2011 Groundwater Monitoring Well Installations and Water Quality Results - Meadowbank Mine, Nunavut. Doc no. 1323-1112210099, Ver. 0, 10 p., December 15, 2011.

Golder Associates Ltd. (2010). 2010 Groundwater Quality Monitoring Program - Meadowbank Mine. Doc. no. 1207. Project no. 10-1428-0006, 55 p., December 17, 2010.

Golder Associates Ltd. (2009). 2009 Groundwater Quality Monitoring Program - Meadowbank Mine. Doc. no. 957. Project no. 09-1428-0013, 49 p., October 29, 2009.

Golder Associates Ltd. (2008a). Tailings Storage Facility Dike Design Meadowbank Gold Project. Doc. 784. December 2008.

Golder Associates Ltd. (2008b). 2008 Groundwater Quality Monitoring Program - Meadowbank Mine. Doc. No. 801, V.0. Project no. 08-1428-0008. 51 p., January 14, 2008.

Golder Associates Ltd. (2007). Pit slope design criteria for the Portage and Goose island deposits. Doc. No. 06-1413-089/5000. 173 p., April 5, 2007

Golder Associates Ltd. (2006). Meadowbank Gold Project - 2006 Baseline Groundwater Quality. Doc. No. 317 06-1122-186, 14 p., December 4, 2006.

Golder Associates Ltd. (2005). Technical Memorandum on “Items #24a and 37 - Predictions of Regional Groundwater Flow Directions after mine Closure,” October 2005.

Golder Associates Ltd. (2004a). Predictions of brackish water upwelling in open pits - Meadowbank Project. March 12, 2004.

Golder Associates Ltd. (2004b). Predictions of groundwater inflow to open pits - Meadowbank Project. February 6, 2004.

Golder Associates Ltd. (2004c), Report on Hydrogeology Baseline Studies, Meadowbank Gold Project, February 3, 2004.

Golder Associates Ltd. (2003), Report on Permafrost Thermal Regime Baseline Studies, Meadowbank. Project, December 18, 2003.

Golder Associates Ltd. (2002). Factual Report on Geotechnical Drilling, Hydrogeological, and Geophysical Investigations - Meadowbank Project. Report no. 0712, 19 p., July 12, 2002.

Gornitz, V. 1972. Sodium: Element and Geochemistry. In The Encyclopedia of Geochemistry and Environmental Sciences. Ed. R.W. Fairbridge. New York: Van Nostrand Reinhold Co. pp. 1096-1099

Guimera, J., and J. Carrera (2000), A comparison of hydraulic and transport parameters measured in low-permeability fractured media, J. Contam. Hydrol., 41(3 – 4), 261 – 281.

Johnson, A.I. (1967). Specific yield – Compilation of specific yields for various materials U.S. Geological Survey Water-Supply Paper 1662-D, 74 pp

Kachhwal, L.K., Yanful, E.K., Lanteigne, L., 2011. Water Cover Technology for Reactive Tailings Management: A Case Study of Field Measurement and Model Predictions. Water, Air, & Soil Pollution, 214(1-4), 357-382.

Langmuir, D. (1997), Aqueous Environmental Geochemistry, Prentice-Hall, Upper Saddle River, N. J

MEND (2000). 2.15.1a - Flooding of pre-oxidized mine tailings: Mattabi case study

Moncur, M.C., Ptacek, C.J., Lindsay, M.B., Blowes, D.W., Jambor, J.L., 2015. Long-term mineralogical and geochemical evolution of sulfide mine tailings under a shallow water cover. Applied Geochemistry

Nair S. and Pandey P. K., J. (2013). THE ANOVA AND ADSORPTION ISOTHERM STUDY OF ARSENIC REMOVAL USING A COAGULANT OF PLANT ORIGIN WITH FERRIC CHLORIDE. Harmoniz. Res. Appl. Sci. 2013, 1(3), 106-117

O'Kane Consultants (2016). Meadowbank North Cell TSF Expansion – Design of Internal Structures. March 11, 2016.

O'Kane Consultants (2015). TSF North Cell Closure Design Report Construction Plan. 948/1-02, Nov. 16, 2015.

Payne, F.C., Quinnan, J.A. and Potter, S.T. (2008). Remediation hydraulics. CRC Press.

Ravenscroft, P., Brammer, H., Richards, K., (2009). Arsenic Pollution: A Global Synthesis, (RGS-IBG Book Series, Wiley-Blackwell, Chichester, UK, 2009).

Smedley, P., Kinniburgh, D. (2001). Chapter 1. Source and behaviour of arsenic in natural waters. United Nations Synthesis Report on Arsenic in Drinking Water. British Geological Survey, Wallingford, Oxon OX10 8BB, U.K.

SNC-Lavalin (2018a). In-Pit Water Quality Assessment At Closure. Technical report. In-Pit Tailings Deposition Detailed Engineering Study. EPB version issued June 14th, 2018. SNC No.: 651196-2100-4GER-0001. AEM No.: 6118-E-132-001-TCR-002

SNC-Lavalin (2018b) 1D tailings consolidation assessment – In-pit tailings deposition detailed engineering. SLI Ref.no: 651196-2000-4GCA-0001 Rev 01. AEM Ref.no.: 6118-E-132-001-TCR-005. May 3rd, 2018.

SNC-Lavalin (2018c) In-pit tailings deposition thermal modelling – In-pit tailings deposition detailed engineering. SLI Ref.no: 651196-3100-4GER-0001 Rev 00. April 6th, 2018.

SNC-Lavalin (2017a). Preliminary 2D ground thermal modelling – Portage In-Pit Deposition prefeasibility study. Technical Memorandum. 643541-5000-4GCA-0002 Rev PB, July 12, 2017.

SNC-Lavalin (2017b). TSFE Project – In-Pit Tailings Deposition Water Balance and Water Quality Forecast. 643541-5000-40ER-0001, B0B. June 9, 2017.

SNC-Lavalin (2017c). 1D Tailings consolidation modelling assessment – Tailing Storage Portage In-Pit Deposition prefeasibility study. Technical Memorandum. 643541-5000-4GCA-0001 Rev PB, May 31, 2017.

SNC-Lavalin (2016a). TSFE – In-Pit Tailings Deposition Concept. Tailings Storage Facility Extension Project – Phase 2, 637215-1000-4GER-0001. Version A00. November 4, 2016.

SNC-Lavalin (2016b). Multiple Accounts Analysis for the Tailings Storage Facility Extension Project (TSFE) – Final Report. 637215-5000-4GER-0001. Version A00. October 24, 2016.

SNC-Lavalin (2015). Geotechnical investigation Report – Central Dike. Meadowbank Mine. Project no.: 633660 December 22, 2015.

Tanaka, M., Takahashi, Y., Yamaguchi, N., Kim, K.M., Zheng G.D., and Sakamitsu, M. "The difference of diffusion coefficients in water for arsenic compounds at various pH and its dominant factors implied by molecular simulations," Geochimica et Cosmochimica Acta, vol. 105, pp. 360–371, 2013.

Takahashi Y., Sakamitsu M. and Tanaka M. (2011) Diffusion coefficients of arsenate and arsenite in water at various pH. Chem. Lett. 40, 1187–1188

Tetra Tech (2016). Update to pit E3 South Wall Stability Analysis - Meadowbank Mine, Nunavut. 27 p., May 11, 2016.

Vigneault, B., Campbell, P.G.C., Tessier, A, De Vitre, R., 2001. "Geochemical changes in sulfidic mine tailings stored under a shallow water cover". Water Research, 35:1066-1076.

WASY Software, 2005. FEFLOW 6.2 finite element subsurface flow and transport simulation system: user's manual. WASY Institute, Berlin, l92pp.

Willowstick Geophysical Investigation (2015). Meadowbank, South Cell Tailings Pond, Central Dike. Project no. 15198, October 5, 2015.

Xu, M., and Y. Eckstein (1995). Use of weighted least-squares method in evaluation of the relationship between dispersivity and field scale. Ground Water 33(6-10), 16-24.

Appendix A

Additional tables

Table A.1: Calibrated hydraulic conductivity values for hydrogeological modelling

						Calibrated hydraulic conductivity values (m/s)										
Stratigraphy	**Layers**	**Layers elevation**	**Top Elevation (masl)**	**Layer Thickness (m)**	**Till**	**General stratigraphy**	**Bay Fault**	**Bay Fault Splay**	**2nd Portage Fault**	**Central Dump**	**Pit tailings**	**Cells Tailings**	**Fractured bedrock under tailings**	**Goose Contact Qz/UM**	**North Channel fractured zone**	**Dikes**
Overburden	1	variable	140	3	5,0E-06					1,0E-08	1,0E-07	1,0E-07			5,0E-07	1,0E-08
	2	variable	137	2	5,0E-06					1,0E-08	1,0E-07	1,0E-07			5,0E-07	1,0E-08
	3	variable	135	3	5,0E-06					1,0E-08	1,0E-07	1,0E-07			5,0E-07	1,0E-08
	4	variable	132	2	5,0E-06					1,0E-08	1,0E-07		1,1E-03		5,0E-07	1,0E-08
Fractured Bedrock	5	variable	130	3		1,7E-07	6,0E-07	6,0E-07	1,0E-05	1,0E-08	1,0E-07			2,0E-06	5,0E-07	1,0E-08
	6	variable	127	2		1,7E-07	6,0E-07	6,0E-07	1,0E-05	1,0E-08	1,0E-07			2,0E-06	5,0E-07	1,0E-08
	7	variable	125	5		1,7E-07	6,0E-07	6,0E-07	1,0E-05	1,0E-08	1,0E-07			2,0E-06	5,0E-07	
	8	variable	120	4		1,7E-07	6,0E-07	6,0E-07	1,0E-05	1,0E-08	1,0E-07			2,0E-06	5,0E-07	
	9	variable	116	7		1,7E-07	6,0E-07	6,0E-07	1,0E-05	1,0E-08	1,0E-07			2,0E-06	5,0E-07	
	10	variable	109	7		1,7E-07	6,0E-07	6,0E-07	1,0E-05	1,0E-08	1,0E-07			2,0E-06	5,0E-07	
	11	variable	102	7		1,7E-07	6,0E-07	6,0E-07	1,0E-05	1,0E-08	1,0E-07			2,0E-06	5,0E-07	
Competent Bedrock	12	variable	95	7		4,2E-08	6,0E-07	6,0E-07	1,0E-05	1,0E-03	1,0E-07			2,0E-06	5,0E-07	
	13	variable	88	7		4,2E-08	6,0E-07	6,0E-07	1,0E-05	1,0E-03	1,0E-07			2,0E-06	5,0E-07	
	14	variable	81	7		4,2E-08	6,0E-07	6,0E-07	1,0E-05	1,0E-03	1,0E-07			2,0E-06	5,0E-07	
	15	variable	74	7		4,2E-08	6,0E-07	6,0E-07	1,0E-05	1,0E-03	1,0E-07			2,0E-06	5,0E-07	
	16	variable	67	7		4,2E-08	6,0E-07	6,0E-07	1,0E-05	1,0E-03	1,0E-07			2,0E-06	5,0E-07	
	17	fixed	60	7,5		4,2E-08	6,0E-07	6,0E-07	1,0E-05	1,0E-03	1,0E-07			2,0E-06	5,0E-07	
	18	fixed	52,5	6,5		2,7E-08	6,0E-07	6,0E-07	1,0E-05		1,0E-07			2,0E-06	5,0E-07	
	19	fixed	46	1		2,7E-08	6,0E-07		1,0E-05		1,0E-07			2,0E-06	5,0E-07	Pit A
	20	fixed	45	4		2,7E-08	6,0E-07		1,0E-05		1,0E-07			2,0E-06	5,0E-07	
	21	fixed	41	3,5		2,7E-08	6,0E-07		1,0E-05		1,0E-07			2,0E-06		Goose Pit
	22	fixed	37,5	7,5		2,7E-08	6,0E-07		1,0E-05		1,0E-07			2,0E-06		
	23	fixed	30	7,5		2,7E-08	6,0E-07		1,0E-05		1,0E-07			2,0E-06		
	24	fixed	22,5	7,5		2,7E-08	6,0E-07		1,0E-05		1,0E-07			2,0E-06		
	25	fixed	15	7,5		1,8E-08	6,0E-07		1,0E-05		1,0E-07			2,0E-06		
	26	fixed	7,5	3,5		1,8E-08	6,0E-07		1,0E-05		1,0E-07			2,0E-06		
	27	fixed	4	4		1,8E-08	6,0E-07		1,0E-05					2,0E-06		
	28	fixed	0	5,5		1,8E-08	6,0E-07		1,0E-05					2,0E-06		
	29	fixed	-5,5	5,5		1,8E-08	6,0E-07		1,0E-05					2,0E-06		
	30	fixed	-11	4		1,8E-08	6,0E-07		1,0E-05					2,0E-06		
	31	fixed	-15	2		1,8E-08	6,0E-07		1,0E-05					2,0E-06		
	32	fixed	-17	13		1,0E-08	6,0E-07		1,0E-05					2,0E-06		
	33	fixed	-30	15		1,0E-08	6,0E-07		1,0E-05					2,0E-06		Pit E
	34	fixed	-45	15		1,0E-08	6,0E-07		1,0E-05					2,0E-06		
	35	fixed	-60	40		1,0E-08	6,0E-07		1,0E-05							
	36	fixed	-100	50		1,0E-08	6,0E-07		1,0E-05							
	37	fixed	-150	50		1,0E-08	6,0E-07		1,0E-05							
	38	fixed	-200	50		1,0E-08	6,0E-07		1,0E-05							
	39	fixed	-250	50		1,0E-08	6,0E-07		1,0E-05							
	40	fixed	-300	50		1,0E-08	4,0E-08		1,0E-06						max permafrost limit	
	41	fixed	-350	50		1,0E-08	4,0E-08		1,0E-06							
	42	fixed	-400	50		1,0E-08	4,0E-08		1,0E-06							
	43	fixed	-450	50		1,0E-08	4,0E-08		1,0E-06							
	44	fixed	-500	50		1,0E-08	4,0E-08		1,0E-06							
	45	fixed	-550	50		1,0E-08	4,0E-08		1,0E-06							
	46	fixed	-600	50		1,0E-08	4,0E-08		1,0E-06							
	47	fixed	-650	50		1,0E-08	4,0E-08		1,0E-06							
	48	fixed	-700	50		1,0E-08	4,0E-08		1,0E-06							
	49	fixed	-750	50		1,0E-08	4,0E-08		1,0E-06							
	50	fixed	-800	-		1,0E-08	4,0E-08		1,0E-06							

Table A.2: Arithmetic mean 2016 hydraulic heads used for the calibration

ID	X (m)	Y (m)	Z (masl)	Observed Head (m)	Simulated Head (m)	Error^2
750 P1 D	638679.8	7214539.4	88.0	116	115	1
750 P1 E	638679.8	7214539.4	100.0	115	115	0
875 P3 A	638821.5	7214404.8	85.0	120	116	16
875 P3 B	638821.5	7214404.8	65.0	118	117	1
CD_Downstream	638505.0	7214485.0	109.9	115	119	16
GPIT13_PZ2	638843.4	7212163.0	91.6	124	130	36
GPIT13_PZ5	638843.4	7212163.0	29.3	126	130	16
PE3-14A	639025.5	7212976.7	61.4	128	131	9
PE3-14B	639025.5	7212976.7	95.6	120	128	64
Pz190P1A	639355.8	7213857.4	116.7	120	127	49
Pz190P1B	639355.8	7213857.4	121.7	128	126	4
Pz190P1C	639355.8	7213857.4	126.7	129	133	16
Pz26P1A1	638450.1	7212095.3	104.4	121	129	64
Pz26P1A2	638450.1	7212095.3	109.4	123	116	49
Pz26P1B1	638450.1	7212095.3	114.9	122	116	36
Pz26P1B2	638450.1	7212095.3	117.9	122	117	25
Pz490P1A	639361.9	7214144.6	114.1	122	118	16
Pz490P1B	639361.9	7214144.6	119.1	128	102	676
Pz490P1C	639361.9	7214144.6	125.8	132	110	484
SC_Pond	638113.5	7214907.1	117.9	130	130	0

Table A.3 : Water quality forecast (SLI, 2018a) of in-pit tailings pore water, without any water treatment

			Pit A		Pit E		Goose Pit	
PARAMETERS	UNITS	CCME Water Quality GUIDELINES for the Long Term Protection of Aquatic Life (Freshwater)	Overall pit water quality (as predicted by Water Quality Model) Initial Concentration	Criteria exceedance	Overall pit water quality (as predicted by Water Quality Model) Initial Concentration	Criteria exceedance	Overall pit water quality (as predicted by Water Quality Model) Initial Concentration	Criteria exceedance
Chloride	**mg/L**	**120**	**116**	**1**	**141**	**1**	**22**	**0,2**
Fluoride (F)	mg/L	0,12	0,29	2	0,32	3	0,15	1
Sulphate (SO4)	mg SO4/L	n/a	2233	n/a	2584	n/a	435	n/a
Total Cyanide (CNt)	mg/L	n/a	1,780	n/a	3,322	n/a	0,000	n/a
Total N equivalent	mg N/L	0,35	*20,2*	58	*23,2*	66	*4,4*	12
Dissolved Aluminium (Al)	mg/L	0,1	0,153	2	0,175	2	0,036	0
Dissolved Silver (Ag)	mg/L	0,00025	0,00026	1	0,00030	1	0,00016	1
Dissolved Arsenic (As)	**mg/L**	**0,005**	**0,9463**	**189**	**1,1003**	**220**	**0,1508**	**30**
Dissolved Barium (Ba)	mg/L	n/a	0,1913	n/a	0,2219	n/a	0,0366	n/a
Dissolved Cadmium (Cd)	mg/L	0,00004	0,00004	1	0,00005	1	0,00007	2
Dissolved Chromium (Cr)	mg/L	0,001	0,0021	2	0,0024	2	0,0004	0
Dissolved Copper (Cu)	mg/L	0,002	0,922	461	1,055	527	0,177	89
Dissolved Iron (Fe)	mg/L	0,3	1,9	6	2,1	7	0,3	1
Dissolved Lead (Pb)	mg/L	0,001	0,002	2	0,002	2	0,000	0
Dissolved Manganese (Mn)	mg/L	n/a	0,139	n/a	0,158	n/a	0,065	n/a
Dissolved Mercury (Hg)	mg/L	0,000026	0,000017	1	0,000018	1	0,000010	0
Dissolved Molybdenum (Mo)	mg/L	0,073	0,101	1	0,117	2	0,031	0
Dissolved Nickel (Ni)	mg/L	0,025	0,030	1	0,035	1	0,006	0
Dissolved Selenium (Se)	mg/L	0,001	0,006	6	0,006	6	0,003	3
Dissolved Strontium (Sr)	mg/L	n/a	0,478	n/a	0,551	n/a	0,120	n/a
Dissolved Thallium (Ti)	mg/L	0,0008	0,0005	1	0,0005	1	0,0006	1
Dissolved Uranium (U)	mg/L	0,015	0,0016	0	0,0019	0	0,0006	0
Dissolved Zinc (Zn)	mg/L	0,03	0,0038	0	0,0039	0	0,0022	0

Table A.4 : K_d values and calculated retardation factors for selected chemical parameters of reclaim water quality forecast

PARAMETERS	Kd Values (L/kg)	Retardation Factor (unitless) R = 1 + (Bulk Density of Aquifer x Kd)/Aquifer Porosity)
Chloride	**0	**1**
Fluoride (F)	^118	1593001
Sulphate (SO4)	^4	54001
Total Cyanide (CNt)	**9.9	133651
Total N equivalent	**0	1
Dissolved Aluminium (Al)	*2900	39150001
Dissolved Silver (Ag)	**8.3	112051
Dissolved Arsenic (As)	**29	**391501**
Dissolved Barium (Ba)	**41	553501
Dissolved Cadmium (Cd)	^1.97	26596
Dissolved Chromium (Cr)	**19	256501
Dissolved Copper (Cu)	*160	2160001
Dissolved Iron (Fe)	*4900	66150001
Dissolved Lead (Pb)	*2000	27000001
Dissolved Manganese (Mn)	*3600	48600001
Dissolved Mercury (Hg)	**52	702001
Dissolved Molybdenum (Mo)	*410	5535001
Dissolved Nickel (Ni)	^4.38	59131
Dissolved Selenium (Se)	^159	2146501
Dissolved Strontium (Sr)	*1300	17550001
Dissolved Thallium (Ti)	**71	958501
Dissolved Uranium (U)	**5	67501
Dissolved Zinc (Zn)	*19	256501

References:	Based upon Shake Flask Extraction Analysis upon Tailings undertaken by SGS 4 October 2014. Assumed 1 : 3 solids liquid ratio in analysis. Tailings porosity and density based upon Appendix B of Golders. 2017. Whale Tail Pit Project, Laboratory Testing on Process Plant Tailings AEM Document: 6112-E-105-001-REP-002. Technical Memorandum. December 14, 2017
	^Median Kd Values from Site Specific Distribution Co-efficients for Preliminary Modelling Purposes. John L. Daniels, Gautham P. Das. International Conference "Waste Management, Environmental Geotechnology and Global Sustainable Development. (ICWMEGGSD'07 - GzO'07)" Ljubljana, SLOVENIA, August 28. - 30., 2007
	*Kd Values for Sandy Till, Site C, Table 4- Solid/liquid partition coefficients (Kd) for selected soils and sediments at Forsmark and Laxemar-Simpevarp Steve Sheppard, Jeff Long, Barb Sanipelli ECOMatters Inc, Canada Gustav Sohlenius Geological Survey of Sweden (SGU) March 2009
	**Kd Values at pH 6.8, Table 46, Soil Screening Guidance: Technical Background Document. Second Edition. Publication 9355.4-17A. May 1996. United States Environmental Protection Agency. Office of Solid Waste and Emergency Response Washington DC 20460.
Aquifer bulk density (g/cm^3) =	2,7
Aquifer effective porosity (unitless)	0,0002